International Journal of Microstructure and Materials Properties

ISSN online: 1741-8429 - ISSN print: 1741-8410
https://www.inderscience.com/ijmmp

Effects of lubrication on shearing process of electrical silicon steels

Yiwei Zhu, Qiusheng Yan, Jiabin Lu, Biao Tang

DOI: 10.1504/IJMMP.2023.10053403

Article History:

Received:	16 April 2020
Last revised:	18 March 2021
Accepted:	11 July 2022
Published online:	20 January 2023

Effects of lubrication on shearing process of electrical silicon steels

Yiwei Zhu

Faculty of Automotive and Transportation Engineering,
Guangdong Normal University of Technology,
Guangzhou, 510665, Guangdong, China
Email: YiweiZHU@gpnu.edu.cn

Qiusheng Yan* and Jiabin Lu

Faculty of Electromechanical Engineering,
Guangdong University of Technology,
Guangzhou, 510006, Guangdong, China
Email: qsyan@gdut.edu.cn
Email: lujiabin@gdut.edu.cn
*Corresponding author

Biao Tang

China Railway Construction Heavy Industry Corporation Limited,
Changsha, 410100, Hunan, China,
Email: 827462794@qq.com

Abstract: In order to improve the shearing section quality of electrical silicon steels, the shearing force and section quality of oblique-shearing electrical silicon steels were studied under the states of no lubrication, liquid lubrication, and solid lubrication. The shearing contact mechanical model of oblique shearing electrical silicon steels was established to reveal the mechanism of the influence of lubrication on the shearing force in the shearing contact zone. The shearing force, section burr, shear surface rollover, surface hardening and other shearing characteristics were studied by experiments. The analysis showed that during the plate shearing process, the addition of lubrication reduces the friction between the tool and the plate, reduces the plate movement, delays the generation and expansion of cracks, and improves the shearing quality. This study can provide a reference for improving the shearing and machining quality of motor core material.

Keywords: electrical silicon steels; oblique shear; lubrication; fracture surface; surface integrity.

Reference to this paper should be made as follows: Zhu, Y., Yan, Q., Lu, J. and Tang, B. (2023) 'Effects of lubrication on shearing process of electrical silicon steels', *Int. J. Microstructure and Materials Properties*, Vol. 16, No. 4, pp.303–319.

Biographical notes: Yiwei Zhu is working as a Lecturer, School of Automotive and Transportation Engineering, Guangdong Normal University of Technology. He obtained his PhD in Mechanical Engineering with specialisation in advanced manufacturing from the Guangdong University of Technology, China in 2020. The areas of his interest are metal plastic deformation and fracture, motor core processing.

Qiusheng Yan, Doctoral supervisor, is working as a Chief Professor of Guangdong Hong Kong robotics Joint College, Guangdong University of Technology. Engaged in precision and ultra-precision processing of semiconductor materials and precision slitting processing of metal plates.

Jiabin Lu, Doctoral supervisor, is working as a Professor of the School of Mechanical and Electrical Engineering, Guangdong University of Technology. Engaged in material processing mechanism and technology, ultra-precision grinding and polishing processing research.

Biao Tang is working as an Engineer of China Railway Construction Heavy Industry Corporation Limited. He received his MS in Mechanical Engineering from the Guangdong University of Technology, China in 2019. The area of his interest is machine tool fault identification.

1 Introduction

As an essential metallic functional material, electrical silicon steels is extensively used in electric, electronics, and military industries (Rodrigues et al., 2012). Before putting into applications, electrical silicon steels sheets are often machined through shearing, punching (Nakata et al., 1991; Takahashi et al., 2008; Bali and Muetze, 2017), and welding (Wanga et al., 2016; Zhang et al., 2017). The quality of the machined surface affects the mechanical and magnetic properties of the final products (Moses et al., 2000; Weiss et al., 2017).

Research showed that reducing the friction between the tools and the workpiece improves the machining quality (Wang and Yang, 2014). During the punching process, the frictional force significantly influences the morphology and the work-hardening of the workpiece fracture surface, thus further affects the quality of the final product (Zhang and Yang, 2013). Wang et al. (2014) conducted punching experiments and simulations to investigate the frictional behaviours of micro-devices in the punching process and found that the frictional force on the workpiece surface increases, making the surface rough under poor frictional conditions. Mucha (2010) conducted comparative punching experiments on silicon steel with coated and non-coated dies and concluded that the height of the burnish zone on the workpiece increased by over 10% when the frictional coefficient of the tool is low. The effects of the frictional force on the morphology of the fracture surface after punching can be validated through experiments. Wang et al. (2013) utilised the lubricant R68 in hydraulic punching and found that the fracture zone on the fracture surface of the workpiece after punching could be reduced by 40% at most. Additionally, in the blanking process, different frictional forces result in significantly different material deformations, directly affecting the work hardening of the blanked

products (Ramezani and Ripin, 2010). Fu et al. (2016) conducted punching experiments on micro-devices and found that the work hardening of the blanked workpiece without lubrication is more significant than that with lubrication. Li and Zhang (2012) conducted finite element analysis on precise punching and revealed that the increase in frictional force during the punching process results in increased work-hardening of the machined region. However, how frictional force affects the work-hardening of the shear surface on the machined workpiece is scarcely reported.

Lubrication between the tools and the workpiece is one of the major means to reduce friction. In the punching process, various methods (including spraying lubricants, using coated tools, and microstructures) can be applied to reduce friction. Meng et al. (2015) applied high-viscosity lubricants to copper sheets to further improve the frictional conditions of in punching process. As a result, the blanked workpieces were efficiently formed with smooth and clean surfaces. Çöl et al. (2013) applied AlCrN coating on the punching die to decrease the frictional force between the punching die and workpiece and increased the burnish zone of the blanked workpiece. Kitamura et al. (2016) designed punching devices with micro-pits and concluded that with an increased amount of lubricant between the punch and the workpiece, the shear surface of the blanked workpiece was smoother. Although the frictional force is reduced with coated tools and microstructures, the manufacturing and maintenance costs increased accordingly. Therefore, spraying lubricants is currently the more economical and practical method.

The shearing process for sheets is similar to the punching process. Yan et al. (2014) analysed the shearing process of the roll shear disc tool and concluded that the shearing quality decreased sharply with the accelerating wear of the shearing tool, but the in-depth mechanical analysis was not conducted. Meanwhile, the stress-strain state of the sheets directly affects the shearing fracture process. Li et al. (2011) considered how the shearing mechanism and the void growth mechanism affect the fracture with the DF model and conducted tensile and compression experiments with aluminium alloys of different shapes and sizes, but the shearing process under composite conditions was not analysed. Park et al. (2017) measured the strain history during the forming of different materials and analysed the fracture in the complex forming process, but the effects of different strain histories on the macroscopic characteristics of the materials were not explained. Decreasing the frictional force in the shearing process affects the stress-strain state of sheets and further affects the quality of the shear surface. However, the action mechanism of the frictional force in the shearing process of metal sheets has not been systematically investigated. The effects of different lubricants on the morphology of shear surface, the metallographic structures of the plastic deformation zone, and shear forces in the shearing process of electrical silicon steel were investigated to explore the mechanism in which lubrication affects the shearing process. This study is expected to provide a basis for further investigation into the shearing mechanism and optimisation of the technical parameters in the shearing process.

2 Materials and methods

The shearing mechanism of electrical silicon steel is shown in Figure 1. Two straight tools were installed separately on the upper and lower tool carriers. The lower tool was horizontally fixed on the machine, while the upper tool was inclined by the angle of α

relative to the lower tool (as shown in Figure 1(a)). A certain lateral clearance c was left between the upper and lower tool. The shearing process was completed through the rapid motion of the upper tool. In the process, the sheets were subjected to various forces, namely, the elastic, elastic-plastic, and plastic deformations, the initiation and propagation of cracks, and the fracture of the sheets. The shearing process is shown in Figure 1(b).

Figure 1 Shearing machining working principle: (a) arrangement of the disc tool during shearing and (b) the machining process

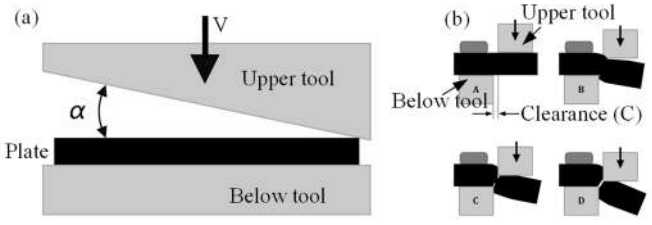

The non-oriented electrical silicon steels MS101 with 0.5 mm in thickness and 60 mm in width was used in the shearing process. The mechanical properties of MS101 are shown in Table 1. The shearing experiments at different velocities were carried out on a KYDJ-400-type precise single-head numerical control (NC) shearing machine (Figure 2) with no lubricants (dry shearing), liquid lubricants (lubricant 25# insulating oil), and solid lubricants (solid lubricant MoS_2). The experimental conditions are shown in Table 2. The tool was washed thoroughly with ethyl alcohol and acetone between each experiment to remove the residual lubricants.

Table 1 Technological parameters

Type	*Thickness/mm*	*Tensile strength/MPa*	*Shear strength/MPa*	*Hardness/HV*
MS101	0.5	451	287	120

Table 2 Experimental conditions of shearing process

Lubrication condition	*Non lubricants; Liquid lubrication* (25# insulating oil); *Solid lubrication* (MoS2)
Lateral clearance/mm	0.025
Shear velocity/mm/s	0.28, 2.8, 28, 280

In order to investigate the difference in the shear forces under different lubrication conditions, a Kistler 5073A three-dimensional dynamometer was used to measure the three-dimensional forces in the shearing process. The directions of the forces are displayed in Figure 2, where F_X is the force parallel to the tool, F_Y is the positive pressure vertical to the tool, and F_Z is the shear force vertical to the sheets.

In order to investigate the difference of shear forces on different lubrication conditions, the three-dimensional forces in shearing process were measured by employing the Kistler 5073A three-dimensional dynamometer and the directions of

forces are displayed in Figure 2. Where, F_X referred to the force whose direction was parallel to the tool direction, F_Y was the positive pressure vertical to the flank of the tool and F_Z was the shear force vertical to the sheets.

Figure 2 Shearing experiment device: (a) precision shearing machine and force measuring instrument; (b) schematic diagram of force measuring direction (see online version for colours)

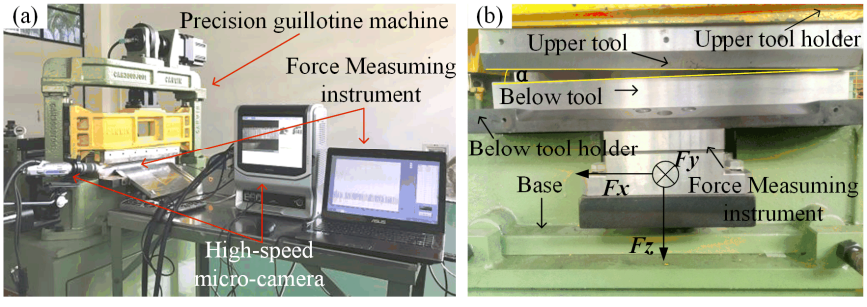

The morphologies of the shear surface of the electrical silicon steel are shown in Figure 3. Various characteristics appeared along the shearing direction and displayed from the top to the bottom as rollover, burnish zone, fracture zone, burr, etc. and then the quality of shear surface can be evaluated according to heights of each of these characteristic bands. The shear surface (Figure 3(a)) was vertically shear by using the wire shearing machine to make up cross section specimens (Figure 3(b)). The specimens were observed and detected in term of the morphology after being embedded and ground. By utilising a Keyence VHX600 microscope with super depth of field, the morphologies of the shear surface and the cross section of the shear specimen were observed in order to measure and record heights of various characteristics bands. By applying a MVK-H3 Vikers microhardness tester, the hardness of the shear cross section was tested under the force of 100 g and held for a time period of 10 s to further evaluate the work hardening state. Additionally, the spacing between measured points and distance to edges of the sheet were both 50 μm and the measured points are shown in Figure 3(b). The mean of 5 times of measurements was taken as the measurement results.

Figure 3 Morphology characteristics of shear section: (a) shear section and; (b) cross section (see online version for colours)

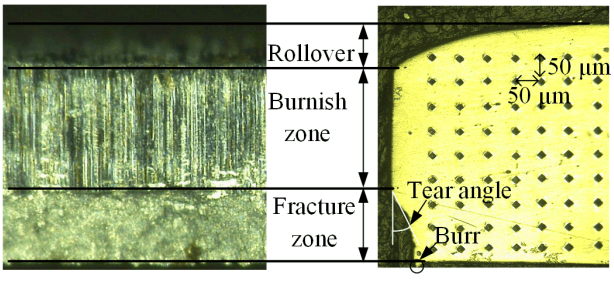

3 Results and discussion

3.1 Shear section morphology under different lubrication conditions

Morphology characteristics of shear surfaces directly reflect the shearing quality. It is speculated that there is a high shearing quality when the burnish zone is large while burrs, fracture zones and rollover are all small in the shear surface (Lo et al., 2007). Figure 4 displays the morphologies of shear surfaces on different lubrication conditions at the shearing speed of 280 mm/s. Great difference existed in the burnish zone on different lubrication conditions, as well as in the fracture zone. The height of burnish zone on the solid lubrication condition was significantly larger than that on conditions of having liquid or no lubricant. When no lubricant was used, there was the lowest height of burnish zone. When having solid lubricant, the burnish zone was even and the interface between the burnish zone and the fracture zone was smooth, showing a favourable quality of shear surfaces. When no lubricant and liquid lubricant were applied, the scratches on the burnish zone were obvious and therefore the burnish zone was rough.

Figure 4 Shear section morphology under different lubrication conditions (shear velocity 280 mm/s): (a) non lubricated; (b) liquid lubrication and (c) solid lubrication (see online version for colours)

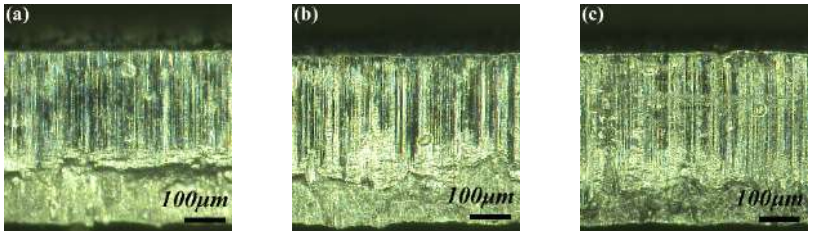

The roughness's of burnish zones were detected by using olympus LEXT OLS 4100 vertical to the shearing direction and the results are displayed in Figure 5. It can be seen from the figure that the surface roughness of the burnish zone on conditions of using lubricants significantly decreased. The mean of surface roughness when adopting liquid lubricant was Ra 1.28 μm, which was 31% lower than that when no lubricant was used. Moreover, the mean of surface roughness when solid lubricant was applied was Ra 1.0 μm, which reduced by 47% compared with that when having no lubricants. It implied that the burnish zone was the most even with the optimal quality when solid lubricant was applied.

Figure 6 shows the morphology of the cross section in shear surface shown in Figure 4. In order to investigate the influence of lubrication conditions on the shear surface, the heights of burnish zones and rollover on the shear surfaces obtained when different lubrication conditions were used were computed. The results are displayed in Figure 7. It can be seen from the figure that at the same shearing speed, the height of burnish zone on shear surface obtained while using solid lubricant was significantly higher than those when liquid lubricant and no lubricant were employed. Moreover, there was the lowest height of burnish zone when no lubricant was applied. With increasing shearing speed, the heights of burnish zones when solid and liquid lubricants were utilised gradually increased.

Figure 5 Burnish zone roughness

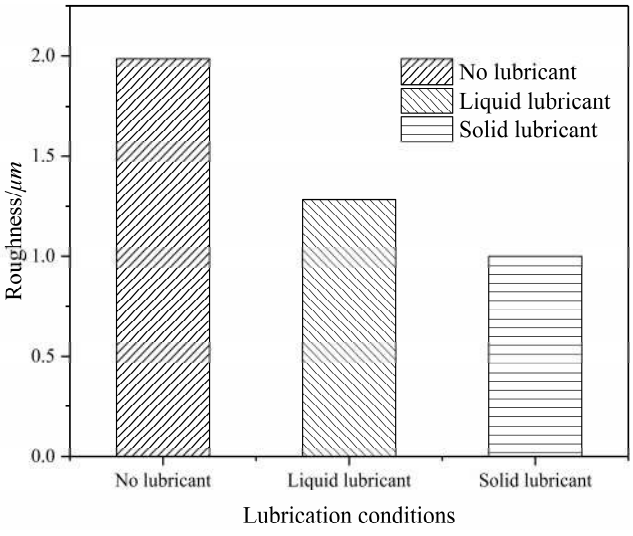

Figure 6 Cross section morphology under different lubrication conditions (shear velocity 280 mm/s): (a) non lubricated; (b) liquid lubrication and (c) solid lubrication (see online version for colours)

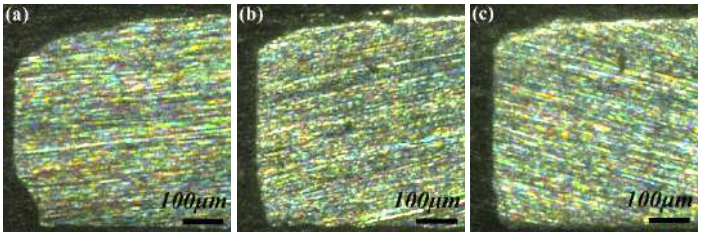

Figure 7 The relationship between the height of characteristic strip and the shear speed under different lubrication (see online version for colours)

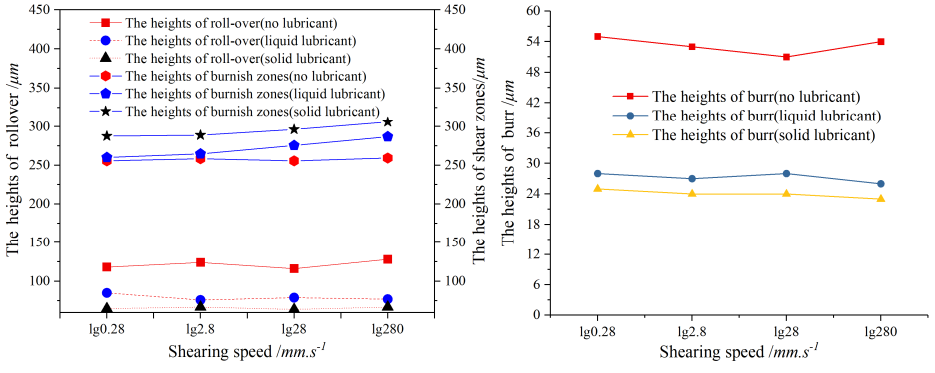

The rollover appeared when solid lubricant and no lubricant were used was in the lowest and highest heights, respectively. On different lubrication conditions, the shearing speed had an insignificant influence on rollover. At four different shearing speeds, the heights

of rollover when no lubricant and liquid lubricant were applied were 122 ± 6 μm and 79 ± 6 μm, respectively. When solid lubricant was adopted, the height of rollover was 66 ± 2 μm, which decreased by about 50% compared with that when having no lubricant.

The burr appeared when solid lubricant and no lubricant were used was in the lowest and highest heights, respectively. On different lubrication conditions, the shearing speed had an insignificant influence on rollover. When solid lubricant was adopted, the height of burr was 24 ± 2 μm, which decreased by about 55% compared with that when having no lubricant.

It can be seen from the aforementioned results that in shearing process, the utilisation of lubricants can significantly influence the morphologies of shear surfaces and improve the shearing quality. Among these conditions, solid lubrication exhibited the optimal effect.

3.2 The microstructure flow of cross-sectional material under different lubrication conditions

Figure 8 displays the metallography of shear cross sections of sheets on different lubrication conditions at the shearing speed of 280 mm/s. It can be seen from Figure 7. that the flows of microstructures on the shearing edges on different lubrication conditions exhibit a similar law. The materials on the shearing edges were all subjected to a great plastic strain, resulting in a great shearing-induced deformation.

Figure 8 Section metallography of cross section under different lubrication conditions (Shear velocity 280 mm/s): (a) non lubricated; (b) liquid lubrication and (c) solid lubrication (see online version for colours)

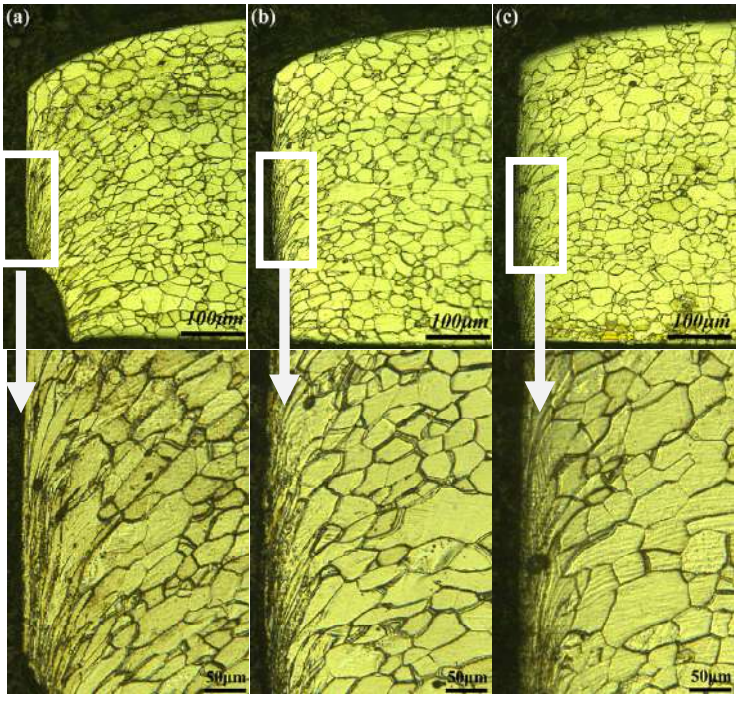

Great difference existed in flow degrees of microstructures and influence area on different lubrication conditions. When no lubricant was used, grains were stretched and therefore the stretched area of grains enlarged, implying it exhibited a more significant change. While using solid lubricant, the deformation zones were more concentrated and only grains on the edges of shear surfaces were subjected to fiberisation deformation.

3.3 Work-hardening under different lubrication conditions

In order to investigate the work-hardening under different lubrication conditions, the hardness of different parts of the shear surface cross-section was measured with an AKASHI MVK-H3 microhardness tester. The hardness nephogram was generated on the data analysis software Origin and presented in Figure 9. The maximum hardness of the shearing edge and the affected area differed significantly under different lubrication conditions. Specifically, the maximum hardness of the edge and the affected area of work-hardening were both at the highest level without lubricant and both at the lowest level with solid lubricant.

Figure 9 Shear edge hardness nephogram under different lubrication conditions (shearing speed 280 mm/s): (a) no lubricant; (b) liquid lubricant and (c) solid lubricant (see online version for colours)

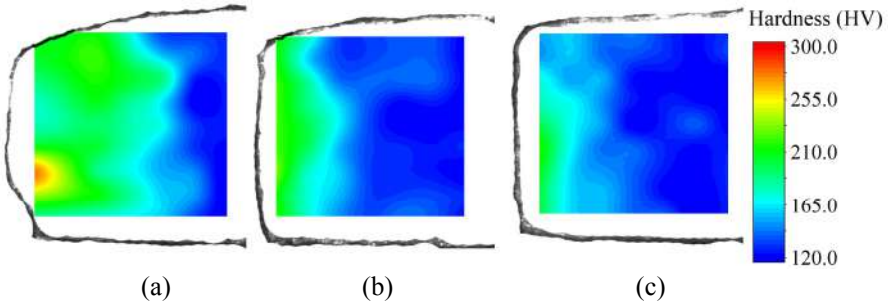

As shown in Figure 10(a), without lubricant, the hardness of the various points on the shearing edge was significantly higher than that with lubricants. The hardness of the different points reached the minimum with solid lubricant. The maximum hardness without lubricant was 280 HV, more than twice the matrix hardness (120 HV). The maximum hardness with liquid and solid lubricants were 220 HV and 210 HV, both less than twice the matrix hardness. Therefore, the materials on the shear surface were subjected to significant deformation in the shearing process, resulting in serious work-hardening. The material deformation and the work-hardening were more significant without lubricant.

According to Figure 10(b), the maximum work-hardening of cross-section and the depth of work-hardening differed significantly under different lubrication conditions. Without lubricant, the depth of work-hardening was about 350 μm and about 250 μm with liquid or solid lubricant. Therefore, the depth of work-hardening significantly decreased with the application of lubricants. Furthermore, the work-hardening with solid lubricant was slightly lower than that with liquid lubricant.

The above results showed that the lubrication between the tool and the sheets directly affects the deformation and work-hardening of the sheets.

Figure 10 Work-hardening under different lubrication conditions: (a) shear edge hardness change and (b) hardness change on the boundary line of the burnish zone and the fracture zone (see online version for colours)

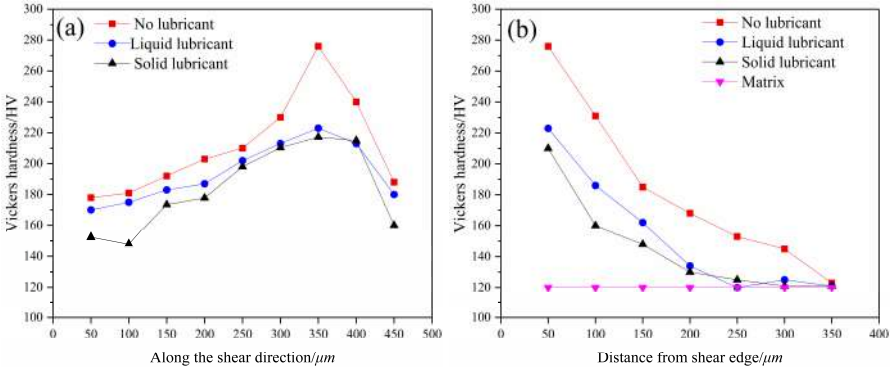

According to the cross-section microstructure flow (Figure 9) and the work-hardening (Figures 9 and 10) under the three lubrication conditions, the work-hardening of the shear surface was closely related to the metallographic structure flow. The larger the plastic deformation of the material, the higher the microscopic slippage and fiberisation of the grains; the greater the microstructure flow, the more significant the work-hardening.

3.4 Iron loss under different lubrication conditions

The iron loss of the samples was measured with the SST method. Figure 11 shows both the iron loss and the deterioration ratio of the samples. The average deterioration ratio of the blanking process is about 15.3%. About 5.7% iron loss could be avoided by optimising the lubrication conditions, which is quite pronounced for energy saving. Hence, the conclusion above is verified and the necessity and feasibility of alleviating the deterioration of the magnetic properties via optimising the lubrication conditions are demonstrated.

Figure 11 Iron loss under different lubrication conditions: (a) iron loss and (b) deterioration ratio (see online version for colours)

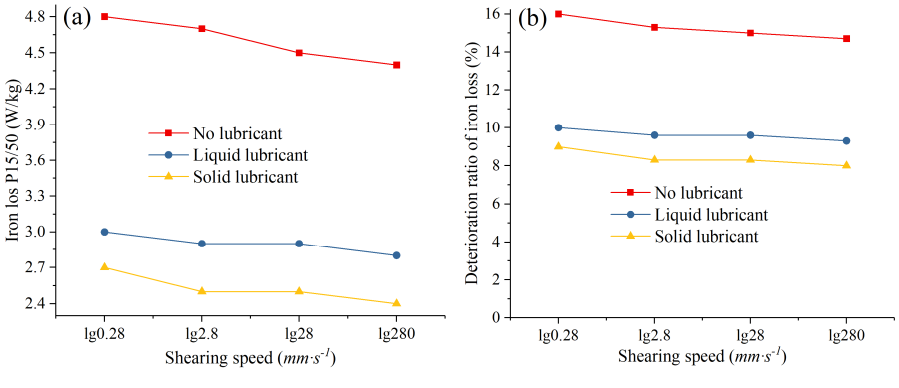

3.5 Shear force under different lubrication conditions

In order to investigate the deformation process of the sheets in the shearing process under different lubrication conditions, the shear force in the shearing process was measured with a Kistler 5073A three-dimensional dynamometer. The X-direction force was a component force generated by the inclination of the shearing edge due to the oblique blade shearing tool, which insignificantly affected the shearing process. Therefore, only forces in Y-direction (positive pressure on the flanks of the sheets) and Z-direction (shear force on the sheets) were taken into account and plotted in Figure 12.

As shown in Figure 12(a), the difference in lubrication conditions significantly affected the acting force F_Y on the flanks of the sheets. F_Y under conditions of no lubricant was significantly larger than that with lubricants. However, F_Y under the conditions of liquid and solid lubricants differed slightly. With the increase of the shearing speed, F_Y under different lubrication conditions increased at first and then decreased. Therefore, F_Y on the flanks of the sheets was related to the lubrication condition, the shearing speed, and the matching between the two parameters. The lateral extrusion force F_Y at a high shearing speed was low, and the lubrication significantly decreased the lateral extrusion force in the shearing process.

Figure 12 The shear force under different lubrication conditions: (a) F_Y and (b) F_Z (see online version for colours)

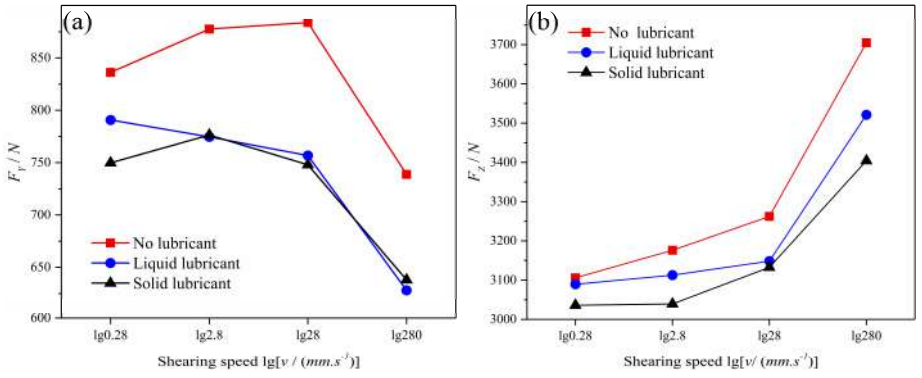

Different lubrication conditions and shearing speeds exert significant influences on the shear force F_Z on the sheets, as shown in Figure 12(b). Without lubricant, F_Z was significantly larger than that with lubricants. The minimum F_Z was measured with solid lubricant. With the increase of the shearing speed, F_Z under different lubrication conditions gradually increased. The higher the shearing speed, the more significant the difference in the shear forces. When the shearing speed was 28 mm/s, F_Z without lubricant and that with solid lubricant was 3262 N and 3131 N, respectively. However, at the shearing speed of 280 mm/s, F_Z rose to 3705 N without lubricant, an increase of 13.5% compared with the F_Z at the shearing speed of 28 mm/s. In this case, with solid lubricant, F_Z grew from 3131 N to 3404 N at the shearing speed of 28 mm/s, an increase of 6% and 302 N lower than that without lubricant. The results showed that the shear force (F_Z) on the sheets was closely related to the lubrication conditions and the shearing speed: the higher the shearing speed, the larger the required shear force on the sheets and the more significant the lubrication effect. The shear force was the smallest with solid

lubricant. Based on the aforementioned experimental results, the shear force significantly decreased after improving the lubrication conditions, and the maximum work-hardening and the affected area significantly decreased while the height of the burnish zone increased. The results indicated that lubrication directly affects the shear force and the stress state of the materials in the deformation process, thus further affects the work-hardening and shearing quality of the shear surface.

4 Lubrication mechanism of the shearing process

In order to investigate the lubrication mechanism in the shearing process, the stress states of the sheets were analysed, as shown in Figure 13. In Figure 13(a), P_{y1} and P_{y2} refer to the lateral pressure of the upper and lower tool on the steel sheets, e.g., the lateral extrusion forces from the flanks of the tool due to the bending deformation of the sheets. P_{z1} andP_{z2} denote the vertical shearing-induced extrusion forces of the upper and lower tool on the steel sheets, which were affected by the shearing parameters and the behaviours of the sheets. μP_{y1} and μP_{y2} (μ refers to the friction coefficient between the tool and the sheets) denote the frictional forces between the flanks of the upper and lower tool and the steel sheets, which were affected by the material matching, the contact state, and the relative motion velocity. μP_{z1} and μP_{z2} represent the frictional forces between the end faces of the upper and lower tool and the sheets. The frictional force can be ignored owing to the low relative displacement between the end faces of the tool and the sheets in the shearing process. Considering the symmetry of shearing, the acting force applied by the upper tool on the steel sheets was the same as that by the lower tool. Therefore, only the acting force of the upper tool was taken into account in the analysis of the stress equilibrium.

Figure 13 Shear model: (a) stress analysis of plate in shear process and (b) boundary lubrication model of tool-plate

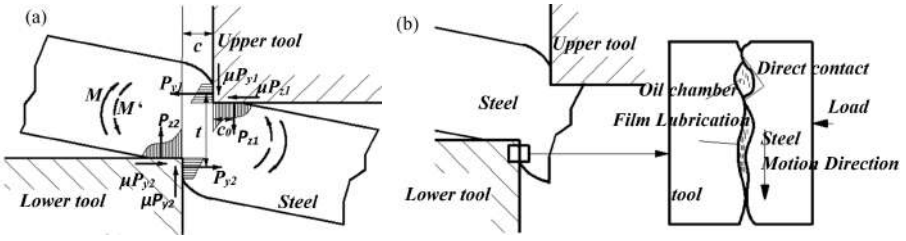

In this context, the stress equilibrium condition of the sheets is as follows:

$$\begin{cases} P_{y1} = P_{y2} \\ P_{z1} + \mu \cdot P_{y1} = P_{z2} + \mu \cdot P_{y2} \end{cases} \tag{1}$$

The torque equilibrium equation can be expressed as follows:

$$P_{z1} \cdot (c + 2c_0) + \mu P_{y1} \cdot c = P_{y1} \cdot t \tag{2}$$

where c, c_0, and t refer to the shearing clearance between the upper and lower tool, the distance from the shear force P_{z1} to the flank of a tool, and the distance between the

extrusion forces (P_{y1} and P_{y2}) of the flanks of the upper and lower tool, which approximated to the thickness of the sheets.

The following formula can be obtained based on formula (2):

$$P_{z1}.(c+2c_0) = p_{y1}.(t-\mu.c) \tag{3}$$

According to formula (2), the bending deformation of the sheets was caused by the shear force P_z of a tool on the sheets and the frictional force μP_y between the sheets and the flank of the tool. The bending deformation of the sheets conformed to the torque equilibrium generated by the extrusion force P_y of the flank of the tool on the sheets: the larger the shear force P_z, the greater the bending deformation of the sheets and the larger the extrusion force P_y of the flank of the tool. According to formula (3), with the other conditions unchanged, the lower the friction coefficient μ between the tool and the sheets, the smaller the frictional force between the sheets and the tool, and the less significant the bending deformation of the sheets and therefore the lower the extrusion force P_y of the flank of the tool.

In the shearing process, the flank of the tool was directly contacted with the surfaces of sheets to generate relative motion, which conformed to the boundary lubrication theory (Bhushan, 2013). The contact states are shown in Figure 12(b). While implementing the shearing process on a certain lubrication condition, the relative slip between the flank of the tool and the sheets was transformed into relative slippage between the molecules of the boundary films or the lubricants. However, the surface frictional forces of the boundary films or the lubricants were far lower than that between the tool and the sheets. Therefore, the friction coefficient significantly decreased. The relative slippage between the molecular layers of the molybdenum disulphide was apt to occur (Najmaei et al., 2015), so the friction coefficient with solid lubricant was slightly lower than that with liquid lubricant. The friction coefficients between the tool and the sheets showed the following relationship under the three frictional conditions:

$$\mu_{dry} > \mu_{liquid} > \mu_{soild} \tag{4}$$

According to formulas (3) and (4), with a constant shear force P_{z2}, the extrusion force P_y of the flank of the tool decreased with the decrease of the friction coefficient; the frictional force μP_y between the tool and the sheets also decreased, resulting in the decrease of the bending deformation of the sheets. Furthermore, the extrusion force P_y of the flank of the tool constantly decreased. Under the three lubrication conditions, the minimum P_y emerged under the solid lubrication condition, followed by that under the liquid lubrication condition, and the maximum P_y emerged without lubricant. However, owing to the friction coefficient under the solid lubrication condition was slightly different from that under the liquid lubrication condition, P_y was slightly different.

Considering that the dynamometer was installed below the carrier of the lowertool, the F_Y and F_Z measured with the dynamometer were as follows:

$$F_Y = P_{y2} \tag{5}$$

$$F_Z = P_{z2} + \mu.P_{y2} \tag{6}$$

According to formula (5), the *Y*-direction pressure measured with the dynamometer was only related to the extrusion force P_y of the flank of the tool, which was directly related to the friction coefficient. Therefore, F_Y reached the minimum and maximum with solid

lubricant and without lubricant. Moreover, the friction coefficient under the liquid lubrication condition was slightly lower than that under the solid lubrication condition. Therefore, F_Y of the former was also slightly lower than that of the latter, which was consistent with the trend of F_Y measured in practice (as shown in Figure 10(a)).

In the shearing process, the shear force P_z was directly correlated with the height of the burnish zone and the work-hardening of the materials. Research showed that P_z increased with the growing height of the burnish zone (Yang and Yuan, 2014). The burnish zone under the solid lubrication condition was higher (as shown in Figure 7). Therefore, P_z under the solid lubrication condition was larger than that under the liquid lubrication condition. The work-hardening of the sheets under the solid lubrication condition was slightly lower than that under the liquid lubrication condition (as shown in Figures 9 and 10). Therefore, P_z under the solid lubrication condition was lower than that under the liquid lubrication condition. However, without lubricant, the work-hardening was much higher. The synergistic effect of the two factors caused the P_z under the solid lubrication condition was the minimum, followed by that under the liquid lubrication condition, and the maximum *Pz* emerged without lubricant. However, the change of P_y had a direct relationship with the friction coefficient. P_z under the solid lubrication condition was lower than that under the liquid lubrication condition. According to formula (6), the comprehensive effect of the three factors resulted in that the minimum and maximum F_Z appeared with solid lubricant and without lubricant, which conformed to the measured results in practice (as shown in Figure 11(b)).

In the shearing process, the materials at the shearing edge of the tool were subjected to bending deformation as being stretched by the shear force F_Z, forming rollover and aggravating the deformation. As the shearing process continued, the work-hardening of the materials in the deformation zone increased. Subsequently, the materials began to fracture and completely separate when microcracks were formed in the materials at the flank near the shearing edge under the effect of tensile force. Finally, the sheets were completely separated when the microcracks were accumulated to a certain degree. Due to the improvement in the lubrication conditions, the scratching on the contact surface and the stress on the materials decreased, resulting in the decrease in the bending deformation of the sheets. Consequently, the formation of microcracks became difficult, and the damage accumulation took a longer time, resulting in the increase in the height of the burnish zone and the decrease of the height of rollover. Additionally, the surface quality improved (Figures 4~7) while the work-hardening decreased (Figures 9 and 10).

5 Conclusions

In the shearing process of sheets, the application of lubricants significantly improves the quality of the shear surface, resulting in the increased height of the burnish zone, the reduction of fracture zone and rollover, and the decreased work-hardening. The solid lubricant has the optimal lubrication effect. At the shearing speed of 280 mm/s, the height of rollover on the shear surface was 46% that without lubricant, the height of burr was 43%that without lubricant, and the height of the burnish zone increased by 19% with solid lubrication. In this case, the depth of work-hardening decreased by 33%, and the maximum work-hardening decreased by 22%.

The application of lubricants led to the reduction of the lateral extrusion force F_Y and the shear force F_Z in the shearing process. In particular, the two forces decreased most

substantially under solid lubrication conditions. With the increase of the shearing speed, F_Y increased first and then decreased while F_Z gradually increased.

The application of lubricants decreased the frictional force between the tool and the sheets in the shearing process and further decreased the flow of sheets. Therefore, the work-hardening and the affected area both significantly decreased. Moreover, the initiation and propagation of cracks were delayed. Therefore, the height of the burnish zone was increased. Hence, the shear surface was more even with favourable surface quality.

About 5.7% iron loss could be avoided by optimising the lubrication conditions, which is quite pronounced for energy saving. Hence, the necessity and feasibility of alleviating the deterioration of the magnetic properties via optimising the lubrication conditions. Thus, this paper provides an in-depth understanding and guidance for reducing the deterioration of magnetic properties caused by the shearing process. This study can provide a reference for improving the shearing and machining quality of motor core material.

Acknowledgements

This work is supported by Scientific Research Initiation Project of Guangdong Polytechnic Normal University (Grant No. 99166990143), Tertiary Education Scientific research project of Guangzhou Municipal Education Bureau (GrantNo.202235355) and National Natural Science Foundation of China (Grant No. 51575112).

Conflict of interests

The authors declare that there is no conflict of interests regarding the publication of this paper.

References

Bali, M. and Muetze, A. (2017) 'Modeling the effect of cutting on the magnetic properties of electrical steel sheets', *IEEE Transactions on Industrial Electronics*, Vol. 64, No. 3, pp.2547–2556.

Bhushan, B. (2013) *Introduction to Tribology*, 2nd ed., Wiley, New York, p.79.

Çöl, M., Kir, D. and Erişir, E. (2013) 'Wear and blanking performance of AlCrN PVD-coated punches', *Materials Science*, Vol. 48, No. 9, pp.514–520.

Fu, M.W., Wang, J.L. and Korsunsky, A.M. (2016) 'A review of geometrical and microstructural size effects in micro-scale deformation processing of metallic alloy components', *International Journal of Machine Tools and Manufacture*, Vol. 109, pp.94–125.

Kitamura, K., Makino, T., Nawa, M. and Miyata, S. (2016) 'Tribological effects of punch with micro-dimples in blanking under high hydrostatic pressure', *CIRP Annals-Manufacturing Technology*, Vol. 65, pp.249–252.

Li, H., Fu, M.W., Lu, J. and Yang, H. (2011) 'Ductile fracture: experiments and computations', *International Journal of Plasticity*, Vol. 27, No. 2, pp.147–180.

Li, J.H. and Zhang, Z.M. (2012) 'Study on work hardening performance for fine-blanking with negative clearance through finite element analysis and experiment', *Journal of Computational and Theoretical Nanoscience*, Vol. 9, pp.1337–1341.

Lo, S.P., Chang, D.Y. and Lin, Y.Y. (2007) 'Quality prediction model of the sheet blanking process for thin phosphorous bronze', *Journal of Materials Processing Technology*, Vol. 194, pp.126–133.

Meng, B., Fu, M.W., Fu, C.M. and Wang, J.L. (2015) 'Multivariable analysis of micro shearing process customized for progressive forming of micro-parts', *International Journal of Mechanical Sciences*, Vol. 93, pp.191–203.

Moses, A., Derebasi, N. and Loisos, G. (2000) 'Aspects of the cut-edge effect stress on the power loss and flux density distribution in electrical steel sheets', *Journal of Magnetism and Magnetic Materials*, Vol. 215, pp.690–692.

Mucha, J. (2010) 'An experimental analysis of effects of various material too*l's Wear on Burr during Generator Sheets Blanking. International Journal of Advanced Manufacturing Technology*, Vol. 50, pp.495–507.

Najmaei, S., Yuan, J., Zhang, J., Ajayan, P. and Lou, J. (2015) 'Synthesis and defect investigation of two-dimensional molybdenum disulfide atomic layers', *Accounts of Chemical Research*, Vol. 48, No. 1, pp.31–40.

Nakata, T., Nakano, M. and Kawahara, K. (1991) 'Effects of stress due to cutting on magnetic characteristics of silicon steel', *IEEE Translation Journal on Magnetics in Japan,* 15 (2, pp.547–550.

Park, N., Huh, H., Lim, S.J., Lou, Y., Kang, Y.S. and Seo, M.H. (2017) 'Fracture-based forming limit criteria for anisotropic materials in sheet metal forming', *International Journal of Plasticity*, Vol. 96, pp.1–35.

Ramezani, M. and Ripin, Z.M. (2010) 'A friction model for dry contacts during metal-forming processes', *International Journal of Advanced Manufacturing Technology*, Vol. 51, pp.93–102.

Rodrigues, D.L., Silveira, J.R.F., Gerhardt, G.J.L., Missell, F.P., Landgraf, F.J.G., Machado, R. and Canpos, M.F. (2012) 'Effect of plastic deformation on the excess loss of electrical steel', *IEEE Transactions on Magnetics*, Vol. 48, No. 4, pp.1425–1428.

Takahashi, N., Morimoto, H. and Yunoki, Y. (2008) 'Effect of shrink fitting and cutting on iron loss of permanent magnet motor', *Journal of Magnetism and Magnetic Materials*, Vol. 320, pp.925–928.

Wang, C., Guo, B. and Shan, D. (2014) 'Friction related size-effect in microforming – a review', *Manufacturing Review*, Vol. 11, No. 23, pp.1–18.

Wang, D. and Yang, H. (2014) 'Advance and trend of friction study in plastic forming', *Transactions of Nonferrous Metals Society of China*, Vol. 24, No. 5, pp.1263–1272.

Wang, J.P., Huang, G.M., Chen, C.C., Ye, Y.C. and Chen, T.T. (2013) 'Investigation of the shear-zone length in fine hydromechanical blanking', *International Journal of Advanced Manufacturing Technology*, Vol. 68, pp.2761–2769.

Wanga, H., Zhang, Y. and Li, S. (2016) 'Laser welding of laminated electrical steels', *Journal of Materials Processing Technology*, Vol. 230, pp.99–108.

Weiss, H.A., Leuning, N., Steentjes, S., Hameyer, K., Andorfer, T., Jenner, S. and Volk, W. (2017) 'Influence of shear cutting parameters on the electromagnetic properties of non-oriented electrical steel sheets', *Journal of Magnetism and Magnetic Materials*, Vol. 421, pp.250–259.

Yan, Q.S., Zhao, X.M., Lu, J.B., Li, Z.R. and Huang, S.W. (2014) 'Wear forms and mechanism of carbide alloy disc tool in disc slitting process for silicon steel sheet', *China Mechanical Engineering*., Vol. 25, pp.508–512.

Yang, Z.Y. and Yuan, H.L. (2011) 'The analysis and study of methods of calculating oblique edge shear force', *Applied Mechanics and Materials*, Vol. 55, pp.2185–2187.

Zhang, D.W. and Yang, H. (2013) 'Numerical study of the friction effects on the metal flow under local loading way', *International Journal of Advanced Manufacturing Technology*, Vol. 68, pp.1339–1350.

Zhang, Y., Wang, H. and Chen, K. (2017) 'Comparison of laser and TIG welding of laminated electrical steels', *Journal of Materials Processing Technology*, Vol. 247, pp.55–63.